The multifragmentation of spectator matter

P.B. Gossiaux, R. Puri, Ch. Hartnack, and J. Aichelin
SUBATECH
Laboratoire de Physique Subatomique et des Technologies Associées
UMR Université de Nantes, IN2P3/CNRS, Ecole des Mines de Nantes
4, rue Alfred Kastler F-44070 Nantes Cedex 03, France.

arXiv:nucl-th/9706038v1 16 Jun 1997

We present the first microscopic calculation of the spectator fragmentation observed in heavy ion reactions at relativistic energies which reproduces the slope of the kinetic energy spectra of the fragments as well as their multiplicity, both measured by the ALADIN collaboration. In the past both have been explained in thermal models, however with vastly different assumptions about the excitation energy and the density of the system. We show that both observables are dominated by dynamical processes and that the system does not pass a state of thermal equilibrium. These findings question the recent conjecture that in these collisions a phase transition of first order, similar to that between water and vapor, can be observed.

I. INTRODUCTION

In semiperipheral reactions of relativistic heavy ions it seems that geometry determines the scenario. The overlapping nucleons of projectile and target form a fireball of high temperature and a density well above normal nuclear matter density. The non overlapping nucleons, called spectators, gain little excitation energy and continue their way with almost the original velocity. This is a conclusion one has drawn from many experiments, first in Berkeley and later at GSI. Whereas the physics of the fireball is pretty well understood that of the spectators is still under debate. Up to now, the most complete experiments of the ALADIN collaboration have shown that the spectator matter disintegrates into many intermediate mass fragments (IMF's). Above 400 MeV/N the fragment multiplicity distribution for a given projectile-target combination does not change anymore. For a for a given projectile the average number of projectile like IMF's as a function of the total bound charge becomes independent of the target [1]. This dependence as well as the fragment multiplicity distribution have been almost perfectly described by a thermodynamical model, advanced by Botvina et al. [2], under the assumption that the excitation energy of the spectator matter is of the order of a couple of MeV/N.

An independent method to measure the excitation energy (or more exactly the temperature) has been employed by the ALADIN collaboration: measuring ratios of isotope yields and assuming that they are produced in thermal equilibrium, one can determine the temperature, which turns out to be about 5 MeV, almost independently of the ratios used. If one displays this temperature as a function of the excitation energy, we observe a functional dependence typical for a first order phase-transition. Consequently, the ALADIN collaboration conjectured that in these reactions a transition from a liquid phase of nuclear matter to a gaseous phase takes place [3].

This temperature of about 5 MeV is in sharp contrast to the one extracted from the slopes of the fragment velocity spectra, measured in the very same experiment. They indeed show a thermal shape but the observed slopes correspond to a temperature of 30 MeV, a value about 6 times larger than that extracted from the particle unstable states or the isotope ratios. Thus it seems that several observables show a functional form as expected for a system in thermal equilibrium but that the temperatures differ by large factors.

Up to now, dynamical models like the Quantum Molecular Dynamics approach (QMD) [4] have not succeeded in describing the data. They underestimate by far the multiplicity of IMF's [5] and have therefore not been considered as reliable despite their success to describe multifragmentation data at low beam energies. The reason for this failure remained obscure because it has been verified that for a given excitation energy a single nucleus disintegrates in QMD simulations into the same number of fragments as in standard statistical models [6]. Thus, one could conclude that in QMD simulations not sufficient energy is transferred to the spectator matter, a puzzling result because the main mechanism for the energy transfer, the elastic NN collisions, are well under control and can be cross-checked by comparison with experimental rapidity distributions.

In QMD calculations each nucleon α moves on a classical trajectory as obtained by a variational solution of the n - body Schrödinger equation:

$$\dot{\vec{p}_\alpha} = -\vec{\nabla}_{\vec{x}_\alpha} \sum_\beta < V(\vec{x}_\alpha, \vec{x}_\beta) > \qquad (1)$$

and

$$\dot{\vec{x}_\alpha} = \vec{p}_\alpha / m. \qquad (2)$$

where $\vec{p}_\alpha$ and $\vec{x}_\alpha$ are the centroids of the Gaussian wave functions (in momentum and coordinate space respectively) which represent the nucleons. $V(\vec{x}_\alpha, \vec{x}_\beta)$ is the two-body interaction between the nucleons. In addition the nucleons interact via stochastic elastic and inelastic NN collisions. For details of the approach we refer to ref. [4].

Recently we advanced a new algorithm [7] for fragment recognition which allows to identify fragments at any time during the reaction. The up to then used Minimum Spanning Tree (MST) method requires the fragments to be well separated from each other in coordinate space, limiting the fragment identification to a very late stage of the reaction only. MST assumes that two nucleons are part of a common fragment if their distance $\sqrt{(\vec{x}_\alpha - \vec{x}_\beta)^2}$ is smaller than $r_C = 3fm$. This new algorithm is called Simulated Annealing Cluster Algorithm (SACA). It searches for that configuration of nucleons and clusters with the largest total binding energy $\sum \zeta_k$, where ζ_k is defined as

$$\zeta_k = \frac{1}{N^f}\left[\sum_{i=1}^{N^f}\frac{(\vec{p}_i - \vec{p}_{cm})^2}{2m} + \frac{1}{2}\sum_{i\neq j}^{N^f} V_{ij}\right]. \qquad (3)$$

provided that $\zeta_k < -4.0$ MeV and $N^f \geq 3$ and as zero otherwise. In this definition, N^f is the number of nucleons in a fragment and $\vec{p}_{cm}$ its center-of-mass momentum. For the technical aspects of this algorithm we refer to [7]. This algorithm has overcome the mathematical difficulties to treat systems of the size of 400 nucleons with a simulated annealing algorithm which limited the similar approach advanced in [8]. It is also similar in spirit to the cluster recognition algorithm advanced by Garcia et al. [9] which, however, does not always find the most bound configuration but may be caught in a local minimum.

This new algorithm allows for new insights into the reaction mechanism, especially into the time dependence of the fragment formation. In fig. 1 we display the time evolution of different observables for the reaction Au + Au 600 MeV/N, b = 8 fm, comparing MST with SACA. This impact parameter has been chosen because it yields the largest IMF multiplicity.

The first row shows the collision rate and the density averaged over the centroids of all nucleons

$$\rho = \frac{1}{N}\sum_{\alpha=1}^{N}\rho(\vec{x}_\alpha) = \frac{1}{N}\sum_{\alpha=1}^{N}\sum_{\beta=1}^{N}(\frac{1}{2\pi L})^{3/2}e^{-(\vec{x}_\alpha - \vec{x}_\beta)^2/2L}$$

with x_α being the centroid position of the nucleon α and L has the standard value of $L = 1.08fm^2$. Please note that in our definition of the density a free particle still has a "self density" of $(\frac{1}{2\pi L})^{3/2} = .32\rho_0$. The second row shows the time evolution of the average mass of the heaviest fragment. According to SACA, it first decreases to a minimum at t = 50 fm/c and re-increases later. Looking in details, one understands that this re-increase is mostly due to the reabsorption of some of the IMF's, as displayed in the third row. At the same time the largest fragment looses nucleons due to evaporation. Hence at the end of the violent phase of the reaction SACA finds that the spectator matter is subdivided into small fragments. They are, however, located in the same space region, as can be seen from the large value of A_{max} obtained by the MST procedure. Nucleons of different fragments interact and proceed towards a thermal equilibrium. The fragments loose their individual identity and merge into a large cluster. Consequently, the size of A_{max} increases.

The persistence coefficient is studied in the last row of fig. 1. This concept has been introduced in [7] as follows: We first define the number of pairs of nucleons in the cluster C at time t $b_C(t) = N_C(N_C - 1)/2$. At a time Δt later, some of the nucleons may have left the cluster and are part of another cluster or singles and others may have entered the cluster. Let N_{C_A} be the number of nucleons which have been in the cluster C at time t and are at $t + \Delta t$ in the cluster A. We define $a_C(t + \Delta t) = \sum_A 0.5 * N_{C_A}(N_{C_A} - 1)$, where the sum goes over all clusters A present at time $t + \Delta t$. The persistence coefficient of the cluster C is now defined as

$$P_C(t + \tfrac{\Delta t}{2}) = a_C(t + \Delta t)/b_C(t) \qquad (4)$$

The mean persistence coefficient for the fragments $2 \leq A \leq 4$ and $4 < A \leq 65$ is displayed in the last row of fig. 1. Its low value as well as the considerable differences between results deduced with SACA and MST (performed at $t > 200fm/c$) indicate that after 60 fm/c the fragments are still very close in coordinate space and exchanging particles. We will come back to this later.

Due to the width L of the Gaussian wave function the expectation value of the two-body potential has a range of 3.6 fm which is large as compared to the range of the nuclear force in free space. One may therefore conjecture that (1) the late thermalization of the spectator matter is due to this large range and therefore fictitious as well as its consequences (late decrease of the number of IMF's,etc.) and (2) that in reality the spectator matter breaks apart into the IMF's observed at t = 60 fm/c. In this article we present results based on this key conjecture.

In figure 2 we display the IMF multiplicity distribution and the size of the largest fragment obtained after 60 fm/c. Both are compared with the experimental data as well as with the results obtained with the MST method at t=200 fm/c. As can be seen, the multiplicity distribution obtained with SACA agrees quite well with the data whereas the MST multiplicity distribution fails completely as already observed in [5].

We proceed now to the dynamical variables. The mean value and the variance of the experimental rapidity distribution of the fragments [10] as a function of the fragment mass are displayed in fig.3. The fragments have a rapidity close to the beam rapidity which is marked by a dashed line. Because the fragment energy spectra look very much like the ones expected from a system

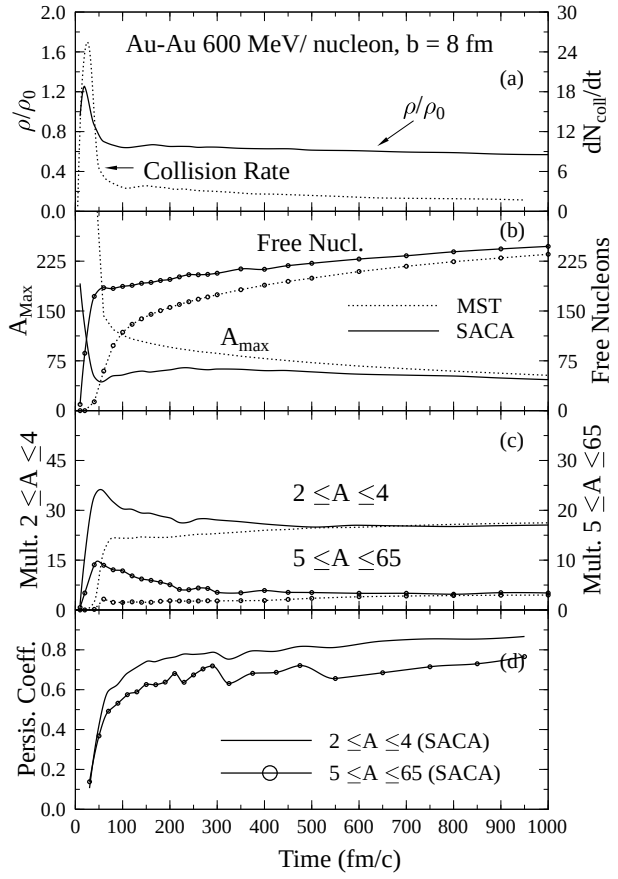

FIG. 1. Evolution of the collision of Au-Au at 600 MeV/N and at an impact parameter of b = 8 fm. From top to bottom the graphs display the time evolution of the density and of the collision rate, of the size of the heaviest fragments and of the number of emitted nucleons, of the multiplicity of fragments with masses $2 \leq A \leq 4$ and with masses $5 \leq A \leq 65$ and of the persistence coefficient.

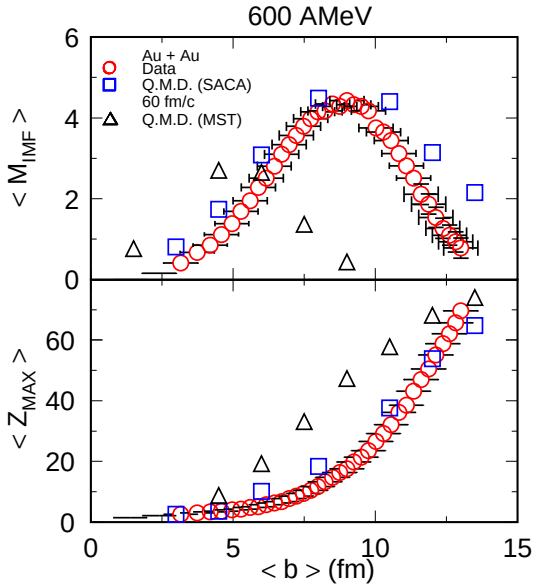

FIG. 2. Multiplicity of IMF's and the charge of the largest fragment as a function of the impact parameter. We show the experimental data [10], the QMD calculation using the minimum spanning tree methods and using SACA at the moment the size of the largest fragment reaches its minimal value, as explained in the text.

in thermal equilibrium and because the variance of the rapidity decreases with the mass number roughly like $\sigma(y) \propto \frac{1}{\sqrt{A}}$ one is tempted to extract a "temperature" $T = \sigma^2(y) \cdot A \cdot m_N$. The value one obtains is about 30 MeV. If one follows the conjecture that multifragmentation is a thermal process one is confronted with the fact that the gas of fragments of a given size A has a 6-8 times higher "temperature" than the spectator matter at the moment the fragments are formed. As only a small fraction of this difference can be attributed to the Coulomb repulsion between the fragments, a yet unknown mechanism is required for heating up the gas of fragments after creation. Such a heating of the system to a temperature of 30 MeV would require more energy than available, as it can be calculated from the kinetic energy of the projectile spectator matter. Furthermore, the high temperature of the fragment kinetic energy spectra raises the question how fragments can survive at all in this hot environment and do not disintegrate into nucleons.

In fig. 3 we display the filtered results of the QMD calculation as well and find that calculation and experiment agree quite well. This is the first time that both the variance of the rapidity distribution and the multiplicity of IMF's have been reproduced by the same theoretical approach, in contrast to the thermal models where both can be individually reproduced, however with vastly different temperatures.

Where does the differences of the apparent temperatures come from? We start our investigation with fig.4 where the time evolution of the average rapidity and of the average transverse momentum in the reaction plane of different classes of projectile-like fragments are displayed. "All nucleons" means that we average over all nucleons which are entrained in fragments of the selected size (which is equivalent to the average over the rapidity or transverse momentum of all fragments of the selected size). "Proj. nucleons" means that we calculate the average value using exclusively the nucleons which have been part of the projectile initially (which is by far the majority). This separation into projectile and target nucleons seems to be impossible as soon as the nucleons have suffered their first collision and quantum mechanics does not allow anymore to determine their origin. However is has been shown recently [11] that, due to the forward-backward enhancement of the NN cross-section, one arrives at the same conclusion if one always names that particle, which is closest to the beam direction, "projectile" nucleon and vice versa. By "Weighted", we mean

that all fragments $A \geq 5$ are taken into account, with their mass A as a weight. We observe that initially the

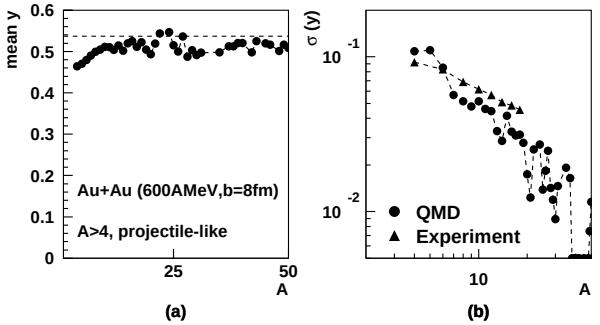

FIG. 3. Mean rapidity and variance of the rapidity distribution as a function of the fragment mass for Au-Au at 600 MeV/N.

projectile nucleons are decelerated substantially. Later the small IMF's are accelerated again. This means that the nucleons which are entrained in the projectile-like fragments have a substantial interaction with the target. If one takes the average over "all nucleons" the deceleration and the acceleration of the IMF's balance each other for the small fragments. The deceleration is caused by the interaction between projectile and target whereas the acceleration is caused by the interaction of the projectile-like fragments with the rest of the projectile-like spectator matter. The smaller the fragments the more probable they are produced close to the projectile-target interface and the more they are decelerated (by potential interaction or by absorbing a target nucleon). Later, the spectator matter, which is less decelerated, re-accelerates these fragments. In fact, the acceleration is more pronounced for small fragments which are produced close to the intersection and have suffered a larger deceleration than the larger fragments. On the other hand, the small fragments are mostly located in the tail and decouple pretty soon (80 fm/c) from the rest of the spectator matter: asymptotically, they remain slower. If one sums over all spectator fragments the average rapidity has to be constant because forces between projectile-like fragments do not change the center-of-mass motion of the projectile-like spectator matter. This is indeed the case as can be seen in the bottom of figure 4.

The average transverse momentum remains very small in the whole process. After the mutual attraction of projectile and target we observe the well known bounce-off caused by the higher density at the interface. As already discussed in ref. [11] the large projectile-like fragments have always a surplus of nucleons which have a transverse momentum pointing away from the target, because those having the opposite direction have a higher change to take part in the fireball. Hence a part of the observed final transverse momentum is due to an initial-time selection of the nucleons and not generated during the interaction. On the average, the light fragments are closer to the projectile-target overlap; therefore, the bounce-off contribution is stronger. Besides, the initial-time contribution is less pronounced because these fragments may also absorb some target nucleons, which must have a strong transverse momentum pointing towards the projectile—in order to entrain it—. The variances of the momen-

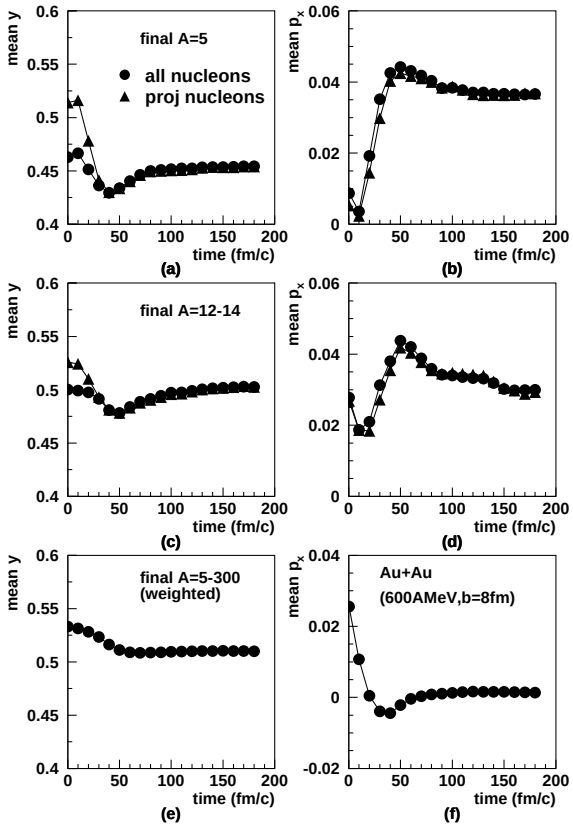

FIG. 4. Evolution of the collision of Au-Au at 600 MeV/N at an impact parameter of b = 8 fm. In the top and middle row we see the mean rapidity and the mean p_x momentum per nucleon of A=5 and A = 12-14 fragments, respectively. The last row display the average over all projectile like fragments.

tum distributions of the fragments are displayed in fig. 5. They are always calculated with respect to the mean values displayed in fig. 4. Regarding "all nucleons" we see, first of all, that the variance for the small fragments as well as that for all fragments changes little in the course of time. Hence, in contradistinction to thermal models, this large variance is there from the beginning and not due to the randomization of collective motion in the course of the approach to thermal equilibrium. The variance of the projectile nucleons changes, however, considerably in the course of time. This is a consequence of the observation that the deceleration and hence the average velocity of the projectile nucleons depends on their transverse distance to the participant region.

If one separates three classes of A=5 fragments accord-

ing to the number of entrained target nucleons one finds a mean rapidity close to $< y >= \frac{n_i \cdot y_{proj} + (5-n_i) \cdot y_{targ}}{5}$ where n_i is the number of projectile nucleons entrained in the projectile like fragment. This can been seen in fig. 6 where we display the mean values and variances for A=5 projectile like fragments, separately for 0, 1 or 2 entrained target nucleons.

We observe that the entrained target nucleons increase the transverse momentum of the fragment. It is obvious from geometry that in order to get entrained in a projectile like fragment the target nucleons must have a positive p_x value. This momentum is added to that caused by the bounce-off, which is around 40 MeV/c.

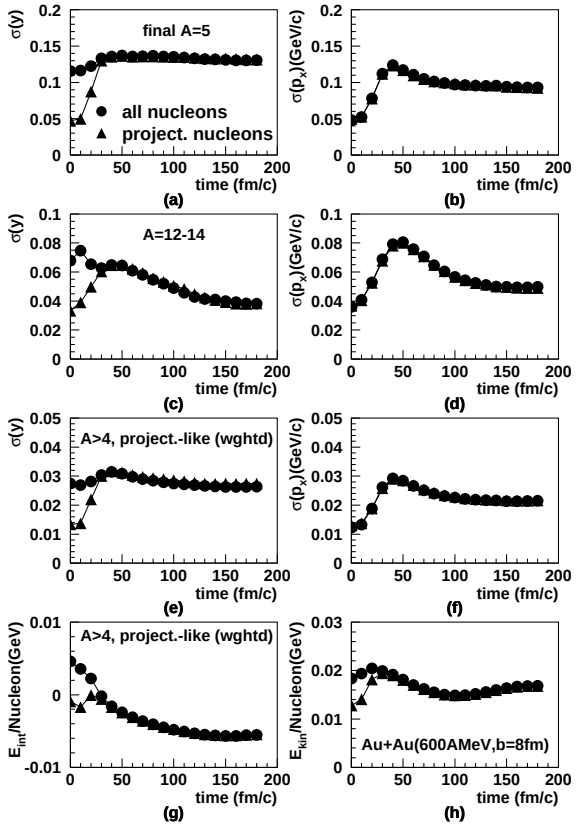

FIG. 5. Evolution of the collision of Au-Au at 600 MeV/N at an impact parameter of b = 8 fm. In the top and second row we see the variances of the rapidity and the p_x momentum distributions of A=5 and A = 12-14 fragments, respectively. The third row displays the average over all projectile like fragments. The last row displays on the left hand side the average internal energy of the fragments and on the right hand side the average kinetic energy of the fragment nucleons in the fragment center of mass system.

The same graph shows also the variances of these dynamical quantities. Assuming that the fragment consists of nucleons which are initially in each direction distributed according to a Gaussian distribution

$$f(p) = (\frac{1}{2\pi\sigma^2})^{1/2} e^{-p^2/2\sigma^2}$$

with $\sigma^2 = \frac{<p^2>}{3} = \frac{p^2_{Fermi}}{5} = 12.5 \times 10^{-3}\ (GeV/c)^2$ we expect $\sigma(y) = .05$ and $\sigma(p_x) = .0469\ GeV/c$. Initially we indeed observe these values for both the transverse momentum and the rapidity and whatever the class considered. Moreover, the large width of the "all nucleons" rapidity distribution of Fig. 5 clearly results from a sum of three distributions, each having a different $< y >$, but the same width $\sigma(y)$.

Once the reaction occurs, the interaction between projectile and target does not only change the mean value but also increases the variance considerably. In other words, this interaction does not affect all nucleons in the same way. Thus we can conclude that the interaction between target and projectile widens the momentum distribution also of those nucleons which are finally entrained in a projectile-like IMF.

In the past the variance of the observed IMF momentum distribution has sometimes been considered as a consequence of an instantaneous breakup of the system. As calculated by Goldhaber [12] the instantaneous break off of fragments of size A from a system of size M yields a Gaussian momentum distribution of these fragments with a mean square momentum of

$$< p^2 >= \frac{3k^2_{Fermi}}{5} A \frac{M-A}{M-1}. \qquad (5)$$

The above discussion has shown that the underlying physics is more complicated than considered in the simple Goldhaber model. Before being part of a fragment the nucleons change their momenta due to the interaction between projectile and target. As we have discussed this interaction leads to an increase of the width of the momentum distribution. Therefore the widths of the momentum distribution found in experiments are systematically larger than those predicted by the Goldhaber formula. A fit of eq. 5 to the ALADIN data [1] yields a Fermi momentum of $k_{Fermi} = 370 MeV/c$ which is about 50 % larger than that extracted from electron scattering.

Despite that quantitative discrepancy the physics behind the Goldhaber model corresponds much more to the result we obtain than the assumption that the system approaches thermal equilibrium. Like in the Goldhaber model we find that the variance of the momentum distribution changes little in the course of the interaction, whereas thermodynamics approaches assume that is it generated by randomizing collective motion. Like in the Goldhaber model we observe that the internal excitation energy of the fragment is almost independent of its center of mass motion, whereas in thermodynamics both are connected by a common temperature. And last, but not least, we see that an important part of the variance of the momentum distribution is due to the initial Fermi motion

in a cold nucleus at zero temperature whereas the thermodynamical models assume that at zero temperature the nucleons have also zero velocity.

The last row of fig. 5 displays on the left hand side the average total energy/nucleon E_{int}/N of the cluster. It is defined in eq. 3. For negative values E_{int}/N corresponds to the binding energy per nucleon. Initially the value of E_{int}/N for those fragments consisting of projectile nucleons only is - 1.55 MeV (as compared to -6.85 average binding energy of the projectile nucleons) because the nucleons which finally belong to a given fragment are not very close in coordinate space and therefore the potential energy is not very high. If we include the fragments which contain target-like nucleons, this mean value increases to +5 MeV. When the violent phase of the reaction is over this value has decreased to -3 MeV. This means that the target like nucleons which are finally entrained in the projectile-like fragments have suffered collisions which have placed them in momentum space close to the projectile nucleons with whom they will form a fragment. At the moment the fragments are formed their binding energy is about 4.5 MeV/N lower than that of the ground state. For matter of comparison with the experimental data we apply the Fermi gas formula (although the system is not in equilibrium) and obtain with $a = 0.15MeV^{-1}$ an apparent temperature of "T" $= \sqrt{E/a} = 5.5MeV$. This is almost exactly the value one extracts for the internal temperature of the IMF's from the experimental isotope ratios or from the experimentally observed populations of particle unstable states as compared to the ground state.

The right hand side of the last row displays

$$< E_{kin}/N >=< \frac{1}{N^f}\left[\sum_{i=1}^{N^f}\frac{(\vec{p}_i-\vec{p}_{cm})^2}{2m}\right] > \qquad (6)$$

the average kinetic energy of the nucleons belonging to a given cluster. We display the average over all fragments. This quantity is a mixture of the Fermi energy and the system's excitation energy. We see that this quantity changes little and is close to the value one obtains from the Fermi motion ($< E_{Kin}/N > \approx 20MeV$). Consequently, the change of the average energy E_{int}/N displayed on the left hand side is mainly due the fact that the nucleons, which will finally form a fragment, come closer together and hence the potential energy increases.

In conclusion we have shown that at energies around 1 GeV/N IMF's are dominantly formed in semiperipheral reactions. Before the formation the interaction between the projectile and target has considerably changed the momentum distribution of those nucleons which are finally part of projectile-like IMF's. The width of the momentum distribution has increased and the average momentum has decreased.

Nucleons which come close in coordinate *and* momentum space during this first interaction phase between projectile and target may form a fragment. This condition implies that the internal excitation energy remains small. Inversely, nucleons with large relative momenta do not form fragments even if they are close together in coordinate space. Hence *all observables, which are sensitive to the internal excitation energies should display an apparent temperature of about 5 MeV.*

The almost linear dependence of the variance of the center of mass motion of the fragments on the mass shows that the fragment momentum distribution is a convolution of the momentum distribution of the nucleons at the time of fragment formation. Due to the interaction of projectile and target and due to the fact that the average momentum of the fragments depends on the number of target nucleons entrained the width of this distribution at the time of fragment production is larger than initially. Therefore the Goldhaber formula underestimates the mean square momentum of the fragments. Because also thermodynamics predicts a linear dependence of the variance of the momentum distribution on the fragment mass this dependence may be also interpreted in a model which assumes thermal equilibrium of the system. From the mass dependence of the slope one obtains, under this assumption, an apparent temperature of 30 MeV [1].

The QMD simulations, with the conjecture that the true fragment distribution is obtained after 60 fm/c, reproduce quantitatively both observed phenomena, those which are usually connected with a low temperature (multiplicity distribution and internal excitation) as well as those which display a much larger apparent temperature like the kinetic energy distribution of projectile like fragments. This is possible because the system does not pass through a state of thermal equilibrium despite the fact that many observables show a form expected for a system in thermal equilibrium. Whether it reproduces the observed energy independence of the fragment multiplicity is presently under investigation

Acknowledgment: We would like to thank Drs. Müller, Schüttauf and Trautmann for many discussions and for providing us with experimental data of the ALADIN collaboration.

[1] A. Schüttauf et al., Nucl. Phys. **A607** (1996) 457
[2] A.S. Botvina et al., Nucl. Phys. **A584** (1995) 737
[3] J. Pochodzalla et al., Phys. Rev. Lett. **75** (1995) 1040
[4] J. Aichelin, Phys. Rep. **202** (1991) 233.
[5] M. Begemann-Blaich et al., Phys. Rev. **C48** (1993) 610
[6] W.F.J. Müller et al., Phys. Lett **B298** (1993) 27
[7] R. Puri et al., Phys. Rev. **C54** (1996) R 28
[8] C. Dorso and J. Randrup, Phys. Lett. **B301** (1991) 328
[9] J.B. Garcia and C. Cerruti, Nucl. Phys. **A578** (1994) 597
[10] A. Schüttauf, private communication
[11] P.B. Gossiaux and J. Aichelin, Phys. Rev. C, in press
[12] A.S. Goldhaber Phys. Lett. **B53** (1974) 306

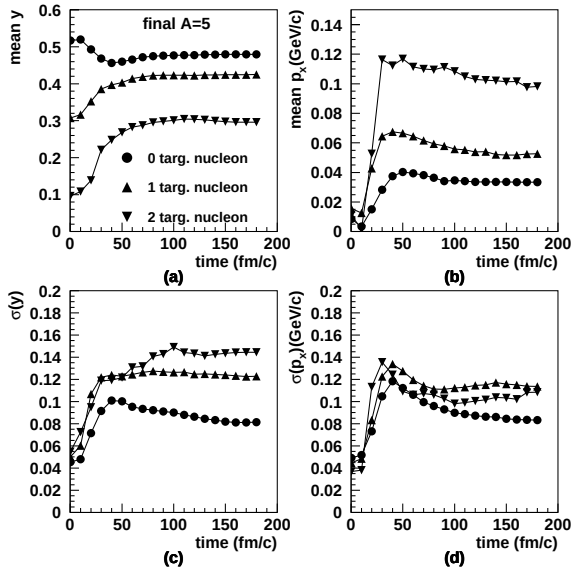

FIG. 6. Evolution of the collision of Au-Au at 600 MeV/N and at an impact parameter of b = 8 fm. We display the mean values and the variances of the rapidity and the in-plane transverse momentum distributions for three different classes of A=5 projectile like fragments.